

Catalytic behavior and synergistic effect of nonthermal plasma and CuO/AC catalyst for benzene destruction

C. He · L. Cao · X. Liu · W. Fu · J. Zhao

Received: 6 May 2014 / Revised: 24 November 2014 / Accepted: 27 January 2015 / Published online: 10 March 2015
© Islamic Azad University (IAU) 2015

Abstract Nonthermal plasma-catalysis hybrid technology (NTP-C) operated at ambient temperature and pressure offers an innovative and effective approach to solving the problem of dilute volatile organic compounds pollution. Herein, the destruction of benzene (50–450 ppm) over an in-plasma NTP-C composite system was investigated. The $\text{AO}_x/\text{active carbon (AO}_x/\text{AC)}$, $\text{AO}_x/3\text{A molecular sieve (AO}_x/\text{MS)}$, and $\text{AO}_x/\gamma\text{-Al}_2\text{O}_3$ (A = Fe, Ag, Zn, Mn, and Cu) catalysts were prepared by the incipient-wetness impregnation method. The destruction performances of NTP alone and NTP-C are compared under different reaction conditions, such as inlet reactant concentration, catalyst type, and energy density. AC exhibits the best benzene removal efficiency among three catalyst supports, and the performances of AO_x/AC under different conditions follow the trend of $\text{CuO/AC} > \text{MnO/AC} > \text{MnO}_2/\text{AC} > \text{Fe}_2\text{O}_3/\text{AC} > \text{AC} > \text{ZnO/AC} > \text{Ag}_2\text{O/AC}$. The NTP with CuO/AC system exhibits the highest benzene elimination capability with almost 90.6 % inlet benzene removed at energy density of 70 and 270 J L^{-1} . The strong adsorption ability of AC and the optimal catalytic ability of crystalline structure of CuO on the AC support may be contributed to the excellent performance of CuO/AC. It is found that the NO_x by-product also can be well controlled over NTP-CuO/AC system. Additionally, the surface of CuO/AC is more slipperier and

homogeneous with the reaction proceeding, indicating higher stability of CuO/AC.

Keywords Nonthermal plasma · Benzene · CuO/AC · Reaction conditions · Synergistic effect

Introduction

Volatile organic compounds (VOCs) are one of the major contributors to air pollution, which can act as the active precursor of photochemical smog, ozone, and organic aerosols. Long-term exposure to VOCs can cause a variety of human diseases, including cancer, cardiovascular, and several insusceptible diseases (Jones 1999). VOC control methods such as thermal combustion, absorption, condensation, biological membrane process, corona discharge, and photocatalytic oxidation may have certain limitations in the aspect of technology and economy for the treatment of low concentration VOCs (<1,000 ppm). Nonthermal plasma (NTP) technique with various advantages as operating at ambient condition, moderate capital cost, compact system, and short reaction time can be more efficient in the elimination of VOCs than the conventional technologies, while some reaction by-products (ozone, NO_x , aerosols, etc.) are inevitably formed during the destruction processes. The synergy of NTP and heterogeneous catalysis (NTP-C) is a promising technology for VOC removal at ambient temperature. Researchers have reported that the NTP-C composite process can greatly reduce the energy consumption, save cost, and improve the biodegradation efficiency (Harling et al. 2008; Gerasimov 2007; Chen et al. 2009). Specially, the quantities of reaction by-products such as aerosols, ozone, and smaller organic compounds are also significantly reduced over NTP-C system (Kim et al. 2005a, b).

Electronic supplementary material The online version of this article (doi:10.1007/s13762-015-0765-6) contains supplementary material, which is available to authorized users.

C. He (✉) · L. Cao · X. Liu · W. Fu · J. Zhao
Department of Environmental Science and Engineering, School of Energy and Power Engineering, Xi'an Jiaotong University, Xi'an 710049, People's Republic of China
e-mail: chi_he@mail.xjtu.edu.cn

Introducing a heterogeneous catalyst affects the chemical activity of the NTP system as the catalyst can change the physical characteristics of the discharge. Roland et al. (2005) have found that short-living active species are formed in the pores of alumina catalyst when exposed to NTP. Durme et al. (2008) have found that some supported metal oxides catalysts have high conversion rates to VOC. The arrangements of NTP-C reactor have two types of configurations [that is, in-plasma catalysis (IPC) and post-plasma catalysis (PPC)], and the performance of the NTP is highly dependent on the configuration used (Kim et al. 2005a, b; Holzer et al. 2005). Compared with PPC, the IPC configuration can improve the VOC purification rate due to micro-discharge phenomena occurred between the catalytic materials poles, and improve the average energy density of high-energy electron in the system (Hensel et al. 2005; Holzer et al. 2005). The IPC technique with dielectric barrier discharge (DBD) packed-bed reactor achieved most attention in recent years (Durme et al. 2008). Many catalyst formulations have been developed and tested, and BaTiO₃, Al₂O₃, SiO₂, TiO₂, MnO₂, and their derivatives are usually adopted in IPC (Sano et al. 2006). It has also been found that the conversion of 100 ppm toluene increases with the discharge voltage at a constant frequency of 200 Hz. From the consideration of maximum light intensity produced by NTP and energy saving, there is an optimal voltage value during the VOC decomposing process (Subrahmanyam et al. 2006). However, there still have some key problems need to be solved although the NTP-C has great advantages for VOCs elimination: the high cost of noble metal loaded catalysts; the synergy effect between catalytic oxidation and plasma is hard to study over laboratorial plasma reactor with small internal volume; and the removal of aromatic hydrocarbons which vast exist in industrial exhaust gases with air as the carrier gas is seldom reported. Moreover, only one or two types of catalysts were included in most of previous studies (Karuppiah et al. 2014; Guo et al. 2010; Zhu et al. 2011; Magureanu et al. 2007; Wallis, et al. 2007; Zhu et al. 2009). From our perspective, different metal oxides and supports have different susceptibilities to reaction parameters as energy density, water vapor, and reactant concentration.

On the basis of the abovementioned issues, an amplified plasma reactor with internal gas space up to about 15 L was employed (meet industrial applications), and benzene (air as the carrier gas) was selected as a representative aromatic hydrocarbon in petrochemical waste gas. The effect of active metal oxides (CuO, MnO, MnO₂, Fe₂O₃, ZnO, and Ag₂O) and supports (AC, γ -Al₂O₃, and MS) on benzene removal efficiency in NTP-C hybrid system is comprehensively studied with the aim of widening the utility of the NTP-C systems in practical industrial situations.

Materials and methods

Chemicals and materials

Commercial coconut shell AC and γ -Al₂O₃ were provided by Henan Xiangyuan water purification material factory, and MS was provided by Sinopharm Chemical Reagent Co., Ltd. Cu(NO₃)₂·3H₂O (AP) was purchased from Tianjin Dibo Chemical Reagent Co., Fe(NO₃)₃·9H₂O (AP) was purchased from Tianjin Tianhe Chemical Co., AgNO₃ (AP) was purchased from Xian Dianli Chemical Co., Zn(NO₃)₂·6H₂O (AP) and C₄H₆MnO₄·4H₂O (CP) were purchased from Tianjin Dengfeng Chemical Reagent Co., and benzene (AP) was purchased from Tianjin Kemiou Chemical Reagent Co. All chemicals were used as received without further purification.

Catalyst preparation

The catalysts used in this work were prepared by incipient-wetness impregnation method, and the metal loading over all catalysts is 5.0 wt%. Typically, the AO_x/AC (A = Mn, Cu, Fe, Zn, and Ag) catalysts were prepared by respective impregnating the AC support with nitrate solutions of MnO₂, CuO, Fe₂O₃, ZnO, and Ag₂O and keeping stationary for 2 h at room temperature. Then, the obtained materials were kept in the high temperature sterilization pot for 5 h under saturate water vapor atmosphere and followed by drying at 80 °C overnight and calcining at 350 °C for 3 h under N₂ stream. The CuO/ γ -Al₂O₃ and CuO/MS were prepared by using the same procedure described above except calcined in the muffle furnace. MnO/AC was prepared by impregnating the supports with manganese nitrate solution. After removal of the excess of water by low-pressure evaporation at 50 °C, the sample was treated at 300 °C for 2 h under N₂ stream.

Catalyst characterizations

X-ray diffraction (XRD) patterns were recorded on a Philips X'Pert powder diffraction system (PANalytic Co., Holland) using Cu K α radiation ($\lambda = 0.15418$ nm) in the 2θ range of 10°–80° (scanning rate of 4° min⁻¹). N₂ adsorption/desorption isotherms of catalysts at 77 K were collected on a SSA-4000 gas sorption analyzer (Biaode Co., China). All samples were degassed under vacuum at 300 °C for 3 h before the measurement. The total pore volume was estimated from the amount of nitrogen adsorbed at a relative pressure (P/P_0) of ca. 0.99. The specific surface area was calculated using the Brunauer–Emmett–Teller (BET) method, and the pore size distribution was derived from the desorption branch of the N₂ isotherm using the Barrett–Joyner–Halenda (BJH) method. The

material on the surface of the catalyst was identified by using TENSOR37 FT-IR analyzer (Bruker Co., Germany). The catalyst was mixed with potassium bromide at a mass ratio of 1:100 and made into tablet, and the spectra were recorded in 4,000–400 cm^{-1} wavelength range. All spectra were collected at a resolution of 4 cm^{-1} with 64 scans. Field emission scanning electron microscopy (FE-SEM) images were recorded on a JSM-6700F microscope (JEOL Ltd., Japan). X-ray photoelectron spectroscopy (XPS) was carried out on a AXIS ULTRA instrument (SHIMADZU, Japan) under high vacuum ($<5 \times 10^{-10}$ torr) using Al $K\alpha$ as the exciting radiation at a constant pass energy of 1,486.6 eV. The C 1 s peak was used to calibrate the binding energy.

Catalytic performance evaluation

The plasma catalysis unit powered by a high voltage and corona discharge was composed of gas and catalyst channels with an inner diameter of 80 mm and length of 300 mm. The passage center had hollow copper discharge electrode with an outer diameter of 20 mm. The surface of tubular discharge electrode was vertically covered with numerous metal filaments as the discharge end. The gas entered from the bottom of reactor and left from the cylinder channel exit at the top. The metal mesh was placed in the cylinder channel to help the catalyst particles evenly disperse in the area between the lining and metal mesh.

Benzene vapor was produced by using the dry air to bubble into flat-bottom flask containing liquid benzene in water bath pot. The benzene concentration depended on the amount of air (adjusting by the mass flowmeter) entering the flat-bottom flask. In addition, there were another two gas streams, one was dehumidification air whose flow and velocity were controlled by the mass flowmeter. The other was used to adjust the relative humidity of gas simulated in the exhaust gas by using the steam generator to produce steam and using the flowmeter to adjust the flow. Above three gas streams were fed into the plasma reactor after evenly mixed in the package. The evaluation system was balanced in the mixture stream for 30 min before turning on the NTP apparatus and starting the NTP-C process. The gas components in the inlet and outlet of the plasma reactor were continuously analyzed and used for pollutant removal rate calculation.

The composition of the outlet gas was quantitatively measured with a GC-MS 6890 and 5973 system (Agilent, USA). The emissions were tested by GC-MS under the conditions including the mass spectrometry detector (EI) of 100 eV, the testing pieces in the range of 33–450 amu, interface temperature of 250 °C, ion source temperature of 250 °C, and helium as carrier gas (99.999 %). The retention time was 35 min, and the initial temperature was

20 °C (kept for 3 min) and then went up to 250 °C at a speed of 10 °C \cdot min $^{-1}$ (kept for 10 min). The exhaust gas collected with KBr window gas pool was tested under the specific working conditions. The NO_x as by-product was measured using the TY2000 flue gas analyzer (Minghua Co., China). The concentration of benzene in reaction process was measured on-line with a PGM-7600 VOCs detector (RAE Systems Co., USA). The benzene conversion was calculated as follows:

$$\eta = \frac{C_0 - C_1}{C_0} \times 100\%$$

where η —the benzene conversion (%); C_0 —the initial concentration of benzene (mg L^{-1}); C_1 —the outlet concentration of benzene (mg L^{-1}).

Discharge power consumptions were measured by a V-Q Lissajous method. The discharge power was calculated from the area of V-Q parallelogram by multiplying the frequency. The specific input energy in the plasma reactor was calculated as follows:

$$\text{SIE} = \frac{\rho}{v} \times 60$$

where SIE—the specific input energy (J L^{-1}); ρ —the discharge power (W); v —the gas flow rate (L min^{-1}).

Results and discussion

Physicochemical properties of the synthesized catalysts

X-ray diffraction and N_2 adsorption/desorption

Fig. S1 shows the XRD results of CuO/AC catalyst and bulk CuO, and no diffraction peaks corresponding to CuO (JCPDS No. 80-1268) can be found, probably due to the low Cu content or high dispersion of CuO nanoparticles over AC support. Table 1 displays the specific surface area (S_{BET}), total pore volume (D_v), and average pore diameter (D_p) of CuO/AC and AC. Both CuO/AC and AC possess large S_{BET} exceeding 490 $\text{m}^2 \text{g}^{-1}$, and pure AC support (609.3 $\text{m}^2 \text{g}^{-1}$) has a larger S_{BET} than that of CuO/AC catalyst (493.8 $\text{m}^2 \text{g}^{-1}$). The N_2 adsorption/desorption isotherm of CuO/AC catalyst is shown in Fig. S2. The CDE section of the curve shows that class B hysteresis loop appeared in the P/P_0 range of 0.2–1.0, indicating that the CuO/AC sample exhibited typical IV shape isotherms,

Table 1 Textural properties of AC and CuO/AC

Catalyst	S_{BET} ($\text{m}^2 \text{g}^{-1}$)	D_p (nm)	D_v (mL g^{-1})
AC	609.3	1.22	0.37
CuO/AC	493.8	1.37	0.34



which is consistent to a diameter in the mesoporous range (Sing et al. 1985), indicating that the CuO/AC sample still maintains the mesoporous structure of AC support.

Fourier transform infrared spectroscopy

Figure 1 shows the infrared spectra of CuO/AC and pure AC, and the chemical groups corresponding to frequency bands derived by FT-IR are listed in Table 2. The peak at $1,138\text{ cm}^{-1}$ is the stretching vibration of phenolic C–O. The peak at approximately $3,415\text{ cm}^{-1}$ can be assigned to the stretching vibration of the OH bond of alcohol, phenolic, and carboxylic groups, as well as the elongation of the amino group NH. These groups are associated with

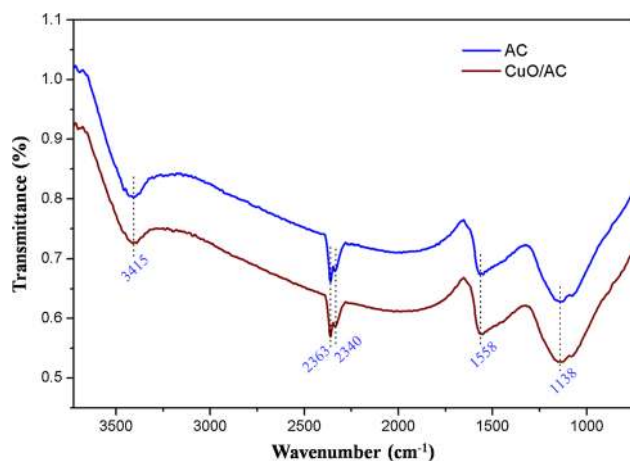
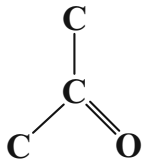
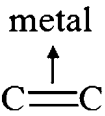
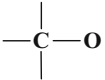


Fig. 1 FT-IR spectra of AC and CuO/AC

Table 2 Chemical groups assignment over CuO/AC catalyst

Wavenumber (cm^{-1})	Molecular fragment	Assignment
3,415		O–H stretching vibration (solid phase)
2,363	S–OH...O	O–H stretching vibrations overtone
2,340	P–OH...O	
1,558	S–OH...O	O–H stretching vibration (solid phase)
	P–OH...O	
1,138		C=C stretching vibration
		C–O stretching vibration

cellulose and proteins of the cell wall biomass (do Nascimento et al. 2014). The peaks at $2,363$ and $2,340\text{ cm}^{-1}$ are related to the stretching vibration of the OH bond of S–OH...O and P–OH...O. The broad region of adsorption around the peak at $1,558\text{ cm}^{-1}$ is attributed to the stretching of C = C bonds (Muzzarelli and Pariser 1978). Most of IR peaks over pure AC are similar with those of CuO/AC sample, indicating that the introduction of CuO phase to AC support has little effect on the performance of AC, and CuO/AC still maintains strong adsorption ability.

X-ray photoelectron spectroscopy

The information of surface composition and chemical state of synthesized catalysts was studied by XPS, as shown in Fig. 2. The survey-scan spectrum in Fig. 2a indicates that the sample consists mainly of the elements Cu and C. The obvious C 1s peak mainly belongs to the AC support and carbon attaching on the sample powders during the XPS measurement. Figure 2b displays the Cu 2p XPS spectra of 5.0 wt% CuO/AC catalyst. The binding energies at around 934.6 and 955.6 eV are, respectively, corresponding to the principal peak and satellite peak of CuO species, indicating the presence of Cu^{2+} . The weak shake-up peak at 940–948 eV and the peak at binding energy of 932.5 eV suggest the existence of reduced copper species (Av-gouropoulos and Ioannides 2003). As is known, the Cu $2p_{3/2}$ binding energy cannot distinguish the Cu^+ and Cu^0 as they are essentially identical. Thus, the Cu LMM Auger lines were further investigated, as shown in Fig. 2c. The

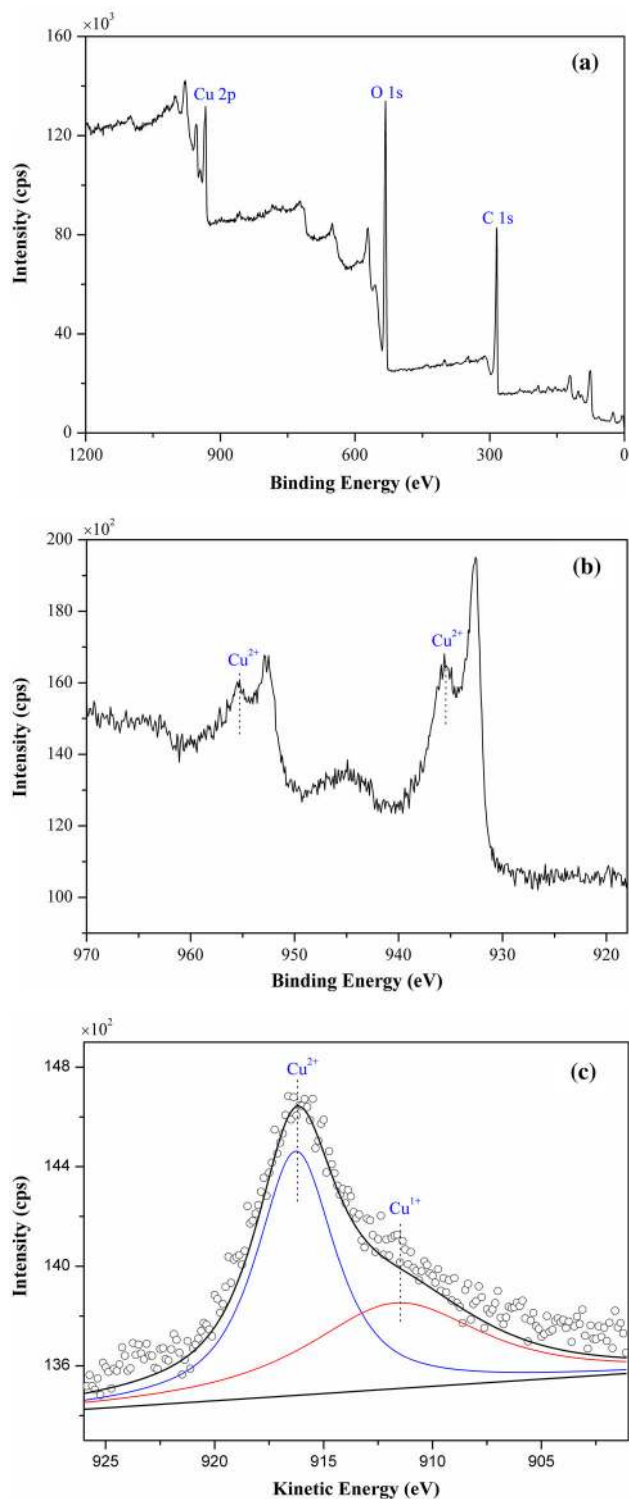


Fig. 2 a The survey, b Cu 2p XPS spectra, and c Cu LMM Auger kinetic energy spectra of CuO/AC catalyst

board feature of the Cu LMM Auger kinetic energy spectra consists of the contribution of two kinds of Cu species. The peaks in the Auger kinetic spectra of 916.6 and 911.5 eV should, respectively, correspond to the Cu^{2+} and Cu^{1+}

species as there are no literature data for metallic copper with such low Auger kinetic energy.

Scanning electron microscopy

Figure 3 presents the SEM images of AC and CuO/AC catalyst. As shown in Fig. 3a, b, the AC has a shaggy and porous surface, which is composed of ball-like and sheet-like nanoclusters with nonuniform size. Lots of micropores with average diameter of 0.5–1.0 μm are distributed in the inner surface of macropore. Above results suggest that the AC is an excellent support with developed porosity, which is beneficial to the benzene adsorption and has good load effect on metal oxides. The CuO/AC catalyst still possesses a porous surface, and the CuO nanoparticles are dispersed evenly on AC surface and do not fill the micropores of AC support (Fig. 3c). In addition, the inner surfaces of macropore are also covered with CuO particles, as shown in Fig. 3d. Information about white nanoclusters (particles seriously aggregated) in the figure is further studied by EDS (Fig. 4), and the result shows that copper has been already loaded on the surface of AC. The atomic ratio of oxygen and copper is about 1:1, indicating that most of copper oxides are in the form of CuO.

Figure 5 presents the SEM images of CuO/AC sample used at various specific input energies (173 and 346 J L^{-1}) for 6 h to illustrate the effect of plasma on catalyst micromorphology. The sample handling with higher energy density presents a relatively slipperier surface than that handling with lower energy density. Furthermore, the size and the distribution of microporous on the surface of CuO/AC are more homogeneous, and the CuO particles are also well distributed. Furthermore, channel collapse appears in the catalyst, which is mainly caused by high energy on catalyst surface. These results infer that when the plasma reactor is combined with CuO/AC, the better performance of the plasma reactor will be achieved under appropriate energy density, which helps AC to maintain excellent adsorption ability.

Benzene destruction over NTP-C system

First of all, the blank tests, that is, NTP alone and NTP combined with three different pure supports, were performed at different benzene inlet concentrations. As shown in Fig. 6, the synergistic effects between NTP and supports can be obviously noticed. For instance, the maximum removal efficiency of benzene (about 35 %) in NTP process is achieved at benzene concentration of 355 ppm, which is corresponding to the minimum conversion rate in the processes of NTP combined with supports. This may be explained that the catalysts help to prolong the benzene retention time in the reactor due to its significant adsorption

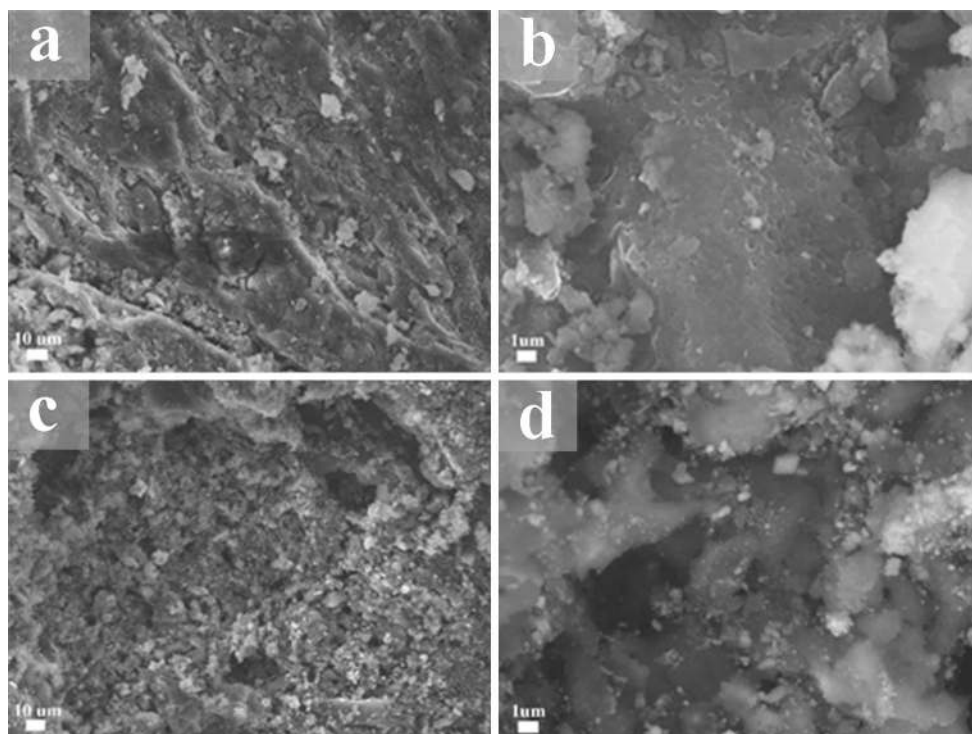


Fig. 3 SEM images of AC (a, b) and CuO/AC (c, d)

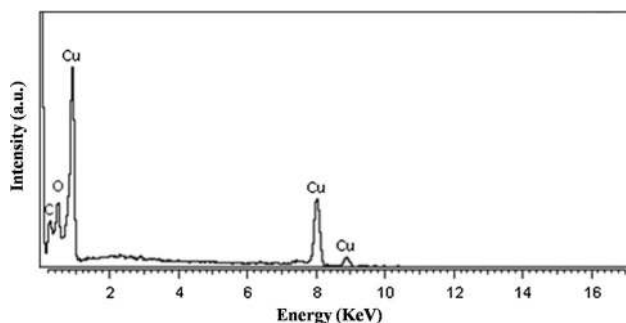


Fig. 4 EDS patterns of CuO/AC catalyst

capacity for pollutant molecules, and as a result, higher collision probability between pollutant molecules and active species enhances the removal efficiency (Vandenbroucke et al. 2011). Besides, the physical properties of a discharge will be affected if a catalyst is introduced into the discharge zone that will lead to a more oxidative discharge (Kim et al. 2004). Introducing a catalyst not only helps to form the short-living active species in the pore volume of porous materials (Roland et al. 2005), but also reduces the concentration of negative ionic species (Chae et al. 2004). Benzene removal efficiency decreases with the increasing of benzene inlet concentration as each absorbed benzene molecule on the catalyst shares fewer electrons and reactive plasma species with the initial benzene concentration

rises. In contrast, benzene removal efficiency gradually increases with the increasing of benzene inlet concentration in single NTP system, and the reason is probably that the initial pollutant concentration rather than the reactive plasma species is the rate-determining step. Benzene removal efficiency in different processes follows the order of $AC > \gamma\text{-Al}_2\text{O}_3 > MS > \text{single NTP}$. The NTP-AC showed 75–85 % benzene removal efficiency in pollutant inlet concentration range of 50–450 ppm, followed by NTP- $\gamma\text{-Al}_2\text{O}_3$ (50–70 %) and NTP-MS (30–50 %). The NTP-AC composite process exhibits the highest benzene removal efficiency due to the developed porous structure as more benzene molecules can be adsorbed and more active species can be generated (Rousseau et al. 2004) and high specific surface area of AC support.

Effect of energy density

The effect of specific input energy (50–300 J L^{-1}) on benzene decomposition in NTP-C composite system was tested, as shown in Fig. 7. NTP with AO_x/AC shows much higher activity for benzene removal than that of NTP with pure AC. The removal efficiency of benzene under different conditions follows the trend of $\text{CuO}/\text{AC} > \text{MnO}/\text{AC} > \text{MnO}_2/\text{AC} > \text{Fe}_2\text{O}_3/\text{AC} > \text{AC} > \text{ZnO}/\text{AC} > \text{Ag}_2\text{O}/\text{AC} > \text{AC}$. NTP with CuO/AC process has the highest benzene removal efficiency among all processes. The

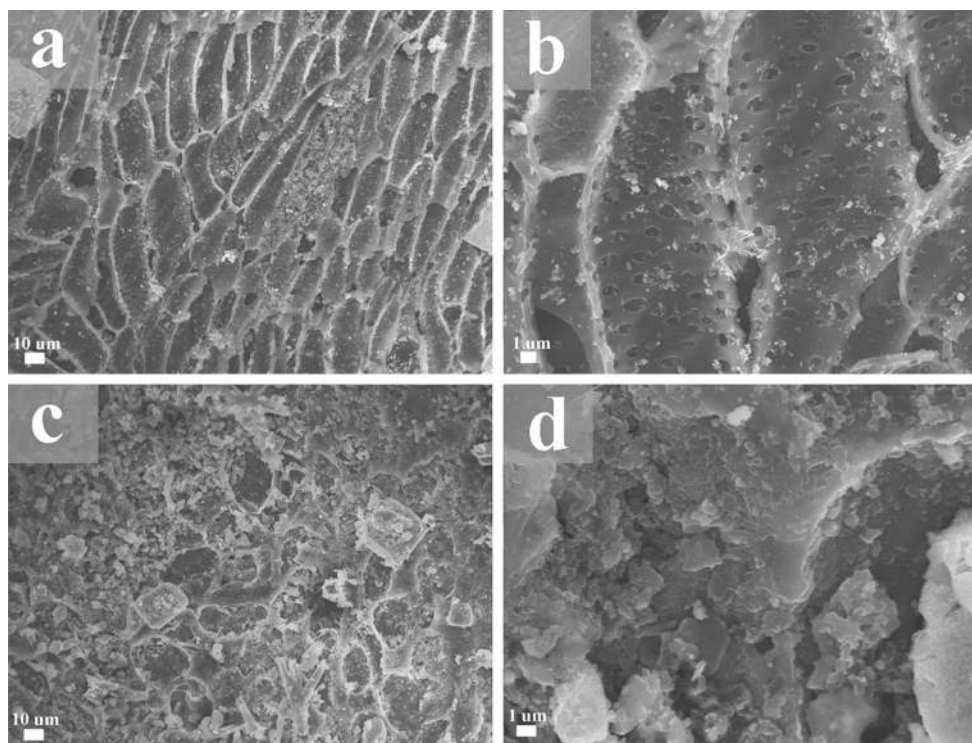


Fig. 5 SEM images of CuO/AC catalyst used at energy density of 173 J L^{-1} (a, b) and 346 J L^{-1} (c, d) for 6 h (conditions: RH = 50 %, gas flow rate = $17,143 \text{ h}^{-1}$, benzene concentration = 250 ppm)

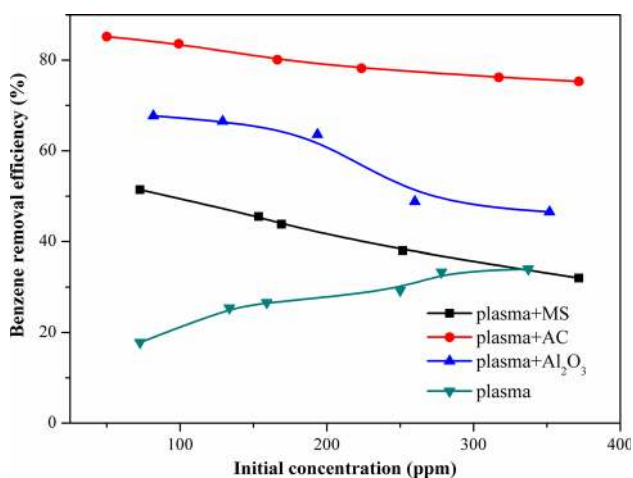


Fig. 6 Influence of benzene inlet concentration and support type on benzene removal (conditions: RH = 50 %, gas flow rate = $18,857 \text{ h}^{-1}$, energy density = 133 J L^{-1} , catalyst dosage = 100 g)

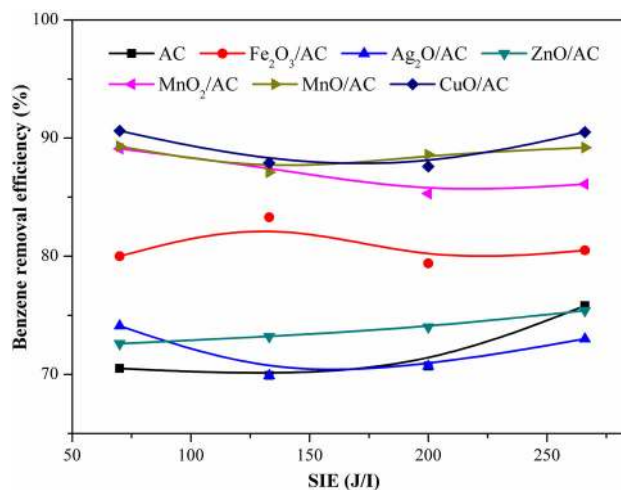


Fig. 7 Influence of energy density and catalyst type on benzene removal (conditions: RH = 50 %, gas flow rate = $18,857 \text{ h}^{-1}$, metal loading = 5.0 wt%, benzene concentration = 240 ppm)

conversion of benzene over CuO/AC can reach almost 90.6 % at energy density of 70 J L^{-1} , much higher than that of pure AC (about 70.5 %). Besides, NTP with MnO/AC and MnO₂/AC also possesses excellent benzene removal capability (>85 %). Noteworthy, there was a worst energy density corresponding to the lowest benzene removal efficiency in various processes, indicating that the

worst value of energy density should be avoided to set as work point in practical industry applications.

Effect of benzene inlet concentration

The effect of benzene inlet concentration on the removal efficiency of NTP-C composite system was further

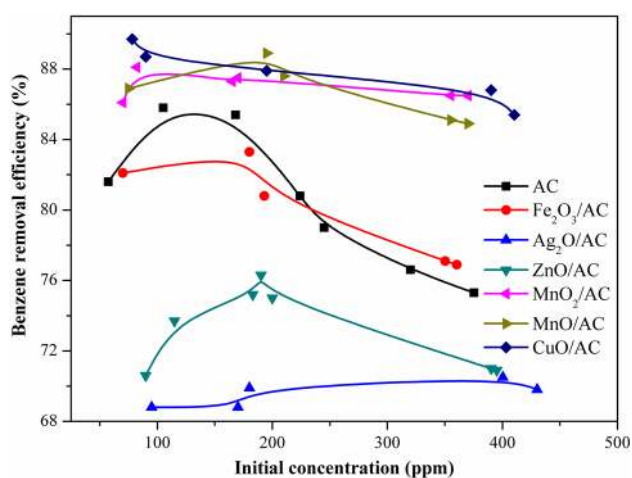


Fig. 8 Influence of benzene inlet concentration and catalyst type on benzene removal (conditions: RH = 50 %, gas flow rate = 18,857 h⁻¹, energy density = 133 J L⁻¹, catalyst dosage = 100 g, metal loading = 5.0 wt%)

investigated. Figure 8 shows that the benzene removal efficiency just has a mild change with the increasing of its inlet concentration from 50 to 500 ppm, indicating that the concentration of benzene has a little effect on the performance of AO_x/CuO for benzene removal in the NTP. The lowest conversion of benzene in this work could reach over 65 %, and the highest could reach about 90 %. Herein, CuO/AC, MnO/AC, and MnO₂/AC show better synergistic effects compared with unmodified AC in the plasma. Figure 8 also reveals that the benzene conversion increases appreciably with the increasing of its inlet concentration from 50 to 200 ppm. As is known, there is competitive adsorption between oxygen and benzene molecules on the active sites during oxidation process, and the surface benzene concentration could be the reaction limiting factor when low contents of organic reagent are introduced, so higher benzene feeding concentration means more chemisorbed benzene molecules, and further lead to a higher benzene construction. However, with the benzene inlet concentrations increase, the surface oxygen concentration gradually becomes the reaction controlling factor, and then, the higher feeding concentration will have adverse effect on the conversion of benzene. Similarly, Corella et al. (2000) and Dai et al. (2008) also found that the trichloroethylene inlet concentration had a positive impact on its catalytic combustion over CeO₂ and Pt-based catalysts.

Effect of catalyst support

The effect of catalyst support on benzene decomposition over NTP-C composite system was further studied, as illustrated in Fig. 9. Obviously, CuO/AC shows the best benzene removal efficiency compared with that of CuO/ γ -

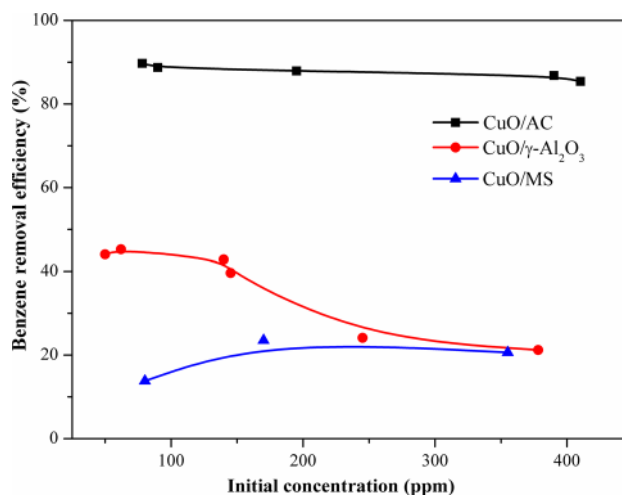


Fig. 9 Influence of benzene inlet concentration and support type on benzene removal (conditions: RH = 50 %, gas flow rate = 18,857 h⁻¹, catalyst dosage = 100 g, metal loading = 5.0 wt%, energy density = 133 J L⁻¹)

Al₂O₃ and CuO/MS. This may be due to the higher specific surface area of AC (609.3 m² g⁻¹) than γ -Al₂O₃ (about 230 m² g⁻¹) (Delagrangé et al. 2006) and MS (about 45 m² g⁻¹) (Simo et al. 2009), leading to the increased active species and stronger adsorption capability of benzene over CuO/AC. Another explanation is that the effect of different supports may lead to different crystalline structure of the loaded catalyst, which is closely related to the catalytic activity. The decomposition of benzene almost reaches 90 % when NTP combined with CuO/AC, and no remarkable change in the whole range of benzene concentration. So the NTP with CuO/AC system could be able to remove benzene waste gases with both lower and higher concentrations.

Effect of catalyst composition on by-product NO_x yield

Abovementioned results reveal that the NTP with CuO/AC, MnO/AC, and MnO₂/AC shows excellent benzene removal efficiencies at different energy densities and benzene inlet concentrations. The performance of a catalyst needs to be evaluated not only by the pollutant degradation rate, but also the by-products yield in the process. NO_x as one of the primary discharge by-products was detected in previous work (Karuppiaha et al. 2012). The production of N and O, the main precursor of NO_x, is related to the dissociation of air. The formation of NO_x occurs when the temperature of the gas is significantly increased by the plasma and reaches about 373 K (Fan et al. 2009). Besides, the type of NO_x strongly depends on the operating conditions such as reactor type, SIE range, temperature, and humidity (Kim et al. 2008). Herein, the NO_x concentrations produced during the processes of NTP combined with CuO/AC, MnO/AC, and MnO₂/AC were tested. As displayed in

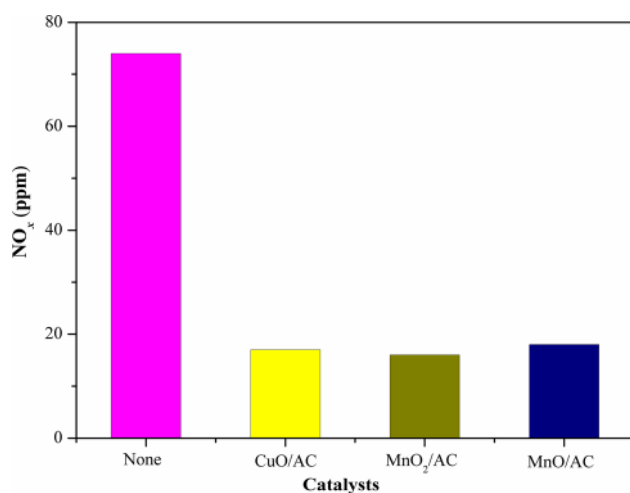


Fig. 10 Distribution of NO_x by-product over NTP-C (C = CuO/AC, MnO/AC, and MnO₂/AC) composite system (conditions: RH = 50 %, gas flow rate = 18,857 h⁻¹, catalyst dosage = 100 g, energy density = 133 J L⁻¹, benzene concentration = 240 ppm)

Fig. 10, the NO_x concentrations in the process of NTP combined with MnO/AC, CuO/AC, and MnO₂/AC modified AC are 12, 11, and 10 ppm, respectively, while the NO_x outcome in single NTP was much higher (48 ppm). The CuO/AC and MnO_x/AC show similar effect for suppressing the NO_x formation.

Conclusion

Benzene removal efficiency increases significantly when catalysts (AC, γ -Al₂O₃, and MS) were introduced into the discharge area, especially for AC, which shows almost 85 % of benzene conversion and increases by 40 % compared with plasma alone. The removal efficiency of benzene further enhances in the presence of metal oxides, and the results show that the CuO/AC exhibits the best performance with almost 90 % of benzene removal. The superiority of benzene destruction over NTP coupled with CuO/AC can be attributed to the high specific area of AC and optimal catalytic ability of crystalline structure of CuO on AC support. The NTP-CuO/AC also shows the lower NO_x production than the NTP alone. The structure and primary surface organic groups of AC have little change after loading with CuO, and the surface properties of CuO/AC further improve with the reaction proceeding. These findings imply that NTP coupled with CuO/AC catalyst is a promising technique for the removal of low concentration VOCs.

Acknowledgments The authors gratefully acknowledge the financial support of the National Natural Science Foundation (21477095, 21403210, 21107106), the Postdoctoral Science Foundation of China

(2014M550498), and the Shannxi Postdoctoral Science Foundation. The authors are also grateful to the reviewers and the editor for their helpful comments.

References

- Avgouropoulos G, Ioannides T (2003) Selective CO oxidation over CuO–CeO₂ catalysts prepared via the urea-nitrate combustion method. *Appl Catal A* 244:155–167
- Chae JO, Demidiouk V, Yeulash M, Choi IC, Jung TG (2004) Experimental study for indoor air control by plasma-catalyst hybrid system. *IEEE Trans Plasma Sci* 32:493–497
- Chen HL, Lee HM, Chen SH, Chang MB, Yu SJ, Li SN (2009) Removal of volatile organic compounds by single-stage and two-stage plasma catalysis systems: a review of the performance enhancement mechanisms, current status, and suitable applications. *Environ Sci Technol* 43:2216–2227
- Corella J, Toledo JM, Padilla AM (2000) On the selection of the catalyst among the commercial platinum-based ones for total oxidation of some chlorinated hydrocarbons. *Appl Catal B* 27:243–256
- Dai QG, Wang XY, Lu GZ (2008) Low-temperature catalytic combustion of trichloroethylene over cerium oxide and catalyst deactivation. *Appl Catal B* 81:192–202
- Delagrange S, Pinard L, Tatibouet JM (2006) Combination of a non-thermal plasma and a catalyst for toluene removal from air: manganese based oxide catalysts. *Appl Catal B* 68:92–98
- do Nascimento GE, Duarte MMB, Campos NF, da Rocha ORS, da Silva VL (2014) Adsorption of azo dyes using peanut hull and orange peel: a comparative study. *Environ Technol* 35:1436–1453
- Durme JV, Dewulf J, Leys C, Langenhove HV (2008) Combining non-thermal plasma with heterogeneous catalysis in waste gas treatment: a review. *Appl Catal B* 78:324–333
- Fan X, Zhu T, Wang M, Li X (2009) Removal of low-concentration BTX in air using a combined plasma catalysis system. *Chemosphere* 75:1301–1306
- Gerasimov G (2007) Modeling study of electron-beam polycyclic and nitropolycyclic aromatic hydrocarbons treatment. *Radiat Phys Chem* 76:27–36
- Guo YF, Liao XB, He JH, Qu WJ, Ye DQ (2010) Effect of manganese oxide catalyst on the dielectric barrier discharge decomposition of toluene. *Catal Today* 153:176–183
- Harling AM, Glover D, Whitehead JC, Zhang K (2008) Novel method for enhancing the destruction of environmental pollutants by the combination of multiple plasma discharges. *Environ Sci Technol* 42:4546–4550
- Hensel K, Katsura S, Mizuno A (2005) DC microdischarges inside porousceramics. *IEEE Trans Plasma Sci* 33:574–575
- Holzer F, Kopinke FD, Roland U (2005) Influence of ferroelectric material and catalysts on the performance of non-thermal plasma (NTP) for the removal of air pollutants. *Plasma Chem Plasma Process* 25:595–611
- Jones AP (1999) Indoor air quality and health. *Atmos Environ* 33:4535–4564
- Karuppiiah J, Reddy EL, Reddy PMK, Ramaraju B, Subrahmanyam C (2014) Catalytic nonthermal plasma reactor for the abatement of low concentrations of benzene. *Int J Environ Sci Technol* 11:311–318
- Karuppiaha J, Reddy EL, Reddy PMK, Ramaraju B, Karvembub R, Subrahmanyama C (2012) Abatement of mixture of volatile organic compounds (VOCs) in a catalytic non-thermal plasma reactor. *J Hazard Mater* 237–238:283–289
- Kim HH, Oh SM, Ogata A, Futamura S (2004) Decomposition of benzene using Ag/TiO₂ packed plasma-driven catalyst reactor:



- influence of electrode configuration and Ag-loading amount. *Catal Lett* 96:189–194
- Kim HH, Ogata A, Futamura S (2005a) Atmospheric plasma-driven catalysis for the low temperature decomposition of dilute aromatic compounds. *J Phys D Appl Phys* 38:1292–1300
- Kim HH, Oh SM, Ogata A, Futamura S (2005b) Decomposition of gas-phase benzene using plasma-driven catalyst (PDC) reactor packed with Ag/TiO₂ catalyst. *Appl Catal B* 56:213–220
- Kim HH, Ogata A, Futamura S (2008) Oxygen partial pressure-dependent behavior of various catalysts for the total oxidation of VOCs using cycled system of adsorption and oxygen plasma. *Appl Catal B* 79:356–367
- Magureanu M, Mandache NB, Parvulescu VI, Subrahmanyam C, Renken A, Kiwi-Minsker L (2007) Improved performance of non-thermal plasma reactor during decomposition of trichloroethylene: optimization of the reactor geometry and introduction of catalytic electrode. *Appl Catal B* 74:270–277
- Muzzarelli RAA, Pariser ER (eds) (1978) Proceedings of the first international conference on chitin/chitosan. MIT Sea Grant Program, Massachusetts Institute of Technology
- Roland U, Holzer F, Kopinke ED (2005) Combination of non-thermal plasma and heterogeneous catalysis for oxidation of volatile organic compounds Part 2. Ozone decomposition and deactivation of gamma-Al₂O₃. *Appl Catal B* 58:217–226
- Rousseau A, Guaitella O, Ropcke J, Gatilova LV, Tolmachev YA (2004) Combination of a pulsed microwave plasma with a catalyst for acetylene oxidation. *Appl Phys Lett* 85:2199–2201
- Sano T, Negishi N, Sakai E, Matsuzawa S (2006) Contributions of photocatalytic/catalytic activities of TiO₂ and Al₂O₃ in nonthermal plasma on oxidation of acetaldehyde and CO. *J Mol Catal A: Chem* 245:235–241
- Simo M, Sivashanmugam S, Brown CJ, Hlavacek V (2009) Adsorption/desorption of water and ethanol on 3A zeolite in near-adiabatic fixed bed. *Ind Eng Chem Res* 48:9247–9260
- Sing KSW, Everett DH, Haul RAW, Moscou L, Pierotti RA, Rouquerol J, Siemieniewska T (1985) Reporting physisorption data for gas/solid systems with special reference to the determination of surface area and porosity. *Pure Appl Chem* 57:603–619
- Subrahmanyam Ch, Magureanu M, Renken A, Kiwi-Minsker L (2006) Catalytic abatement of volatile organic compounds assisted by non-thermal plasma: part 1. A novel dielectric barrier discharge reactor containing catalytic electrode. *Appl Catal B* 65:150–156
- Vandenbroucke AM, Morent R, Geyter ND, Leys C (2011) Non-thermal plasmas for non-catalytic and catalytic VOC abatement. *J Hazard Mater* 195:30–54
- Wallis AE, Whitehead JC, Zhang K (2007) The removal of dichloromethane from atmospheric pressure air streams using plasma-assisted catalysis. *Appl Catal B* 72:282–288
- Zhu T, Li J, Jin YQ, Liang YH, Ma GD (2009) Gaseous phase benzene decomposition by non-thermal plasma coupled with nano titania catalyst. *Int J Environ Sci Technol* 6:141–148
- Zhu T, Wan YD, Li J, He XW, Xu DY, Shu XQ, Liang WJ, Jin YQ (2011) Volatile organic compounds decomposition using non-thermal plasma coupled with a combination of catalysts. *Int J Environ Sci Technol* 8:621–630

